Available online at www.sciencedirect.com
ScienceDirect
Polymer 48 (2007) 245–254
polymer
www.elsevier.com/locate/polymer

Volume phase transition of "smart" microgels in bulk solution and adsorbed at an interface: A combined AFM, dynamic light, and small angle neutron scattering study

Sarah Höfl [a], Lothar Zitzler [b], Thomas Hellweg [a,*], Stephan Herminghaus [c], Frieder Mugele [d]

[a] *Technische Universität (TU) Berlin, Stranski-Laboratorium f. Physikalische und Theoretische Chemie, Strasse des 17. Juni 124, D-10623 Berlin, Germany*
[b] *Universität Ulm, Abteilung Angewandte Physik, D-89069 Ulm, Germany*
[c] *Max-Planck-Institut f. Dynamik und Selbstorganisation, Bunsenstr. 10, 37073 Göttingen, Germany*
[d] *Physics of Complex Fluids, Faculty of Science and Technology, University of Twente, P.O. Box 217, 7500 AE Enschede, The Netherlands*

Received 3 August 2006; accepted 19 October 2006
Available online 21 November 2006

Abstract

In the present article the swelling behavior of copolymer microgel particles made of poly(*N*-isopropylacrylamide)-*co*-vinylacetic acid using dynamic light scattering (DLS), neutron scattering, and in situ atomic force microscopy (AFM) for various copolymerized amounts of vinylacetic acid (VA) (up to 2.5 mol%) under slightly acidic conditions is studied. The transition temperature of these microgel particles is found to be $\approx 32.5 \pm 1$ °C, independent of the VA content. Microgel particles adsorbed onto a solid substrate display a similar volume phase transition as their dissolved counterparts. However, their swelling capacity is reduced by approximately one order of magnitude compared to the bulk value. Nevertheless, the observed effect still is sufficiently large to be exploited for the use of these particles in sensors or as nanoactuators. In addition it can be concluded that the continuous character of the transition observed in solution does not arise from the polydispersity of the particles but can be attributed to the heterogeneity inside each individual microgel particle. Finally, AFM images reveal a pattern on the surface of the collapsed particles, which we attribute to globules formed by collapsed dangling polymer chains. In solution these dangling ends form a brush contributing to the hydrodynamic dimensions of the microgels.

Keywords: Poly(*N*-isopropylacrylamide); Volume phase transition; AFM

1. Introduction

Since the first report on the preparation of poly(*N*-isopropylacrylamide) microgels [1], numerous studies discussing different aspects of these interesting functional polymer materials have been published. The most interesting feature in the behavior of *N*-isopropylacrylamide (NIPAM) based systems certainly is the volume phase transition [2,3]. This phenomenon was already investigated in some detail in macroscopic gels [4–6] and also in different microgels [7–16,44]. A general overview on microgels can be found in Refs. [17,18], or in Ref. [19] with a focus on scattering methods. In macroscopic gels, the volume phase transition can be very slow and in some cases it takes several days until the equilibrium state is reached [20]. Microgels react faster upon changes in temperature, ionic strength, solvent quality, or pH. Therefore, they are well suited to investigate the volume transition. Moreover, due to their colloidal character [21] they are interesting model systems to study processes like formation of mesoscopic crystals [22–26]. Maybe their most visionary potential lies in the possible construction of actuators on the nanometer scale, which are driven by physico-chemical processes like swelling.

In the present study, we describe the properties of poly(*N*-isopropylacrylamide)-*co*-vinylacetic acid (PNIPAM-*co*-VA)

* Corresponding author. Tel.: +49 30 314 22750; fax: +49 30 314 26602.
E-mail address: thomas.hellweg@tu-berlin.de (T. Hellweg).

0032-3861/$ - see front matter © 2006 Elsevier Ltd. All rights reserved.
doi:10.1016/j.polymer.2006.10.026

microgels with different contents of vinylacetic acid. The local structure of the polymer network is studied by means of small angle neutron scattering (SANS). The swelling behavior is investigated by dynamic light scattering (DLS) and moreover by tapping mode atomic force microscopy (AFM). DLS allows to obtain the average degree of swelling in bulk solution, whereas AFM is used to investigate the transition of individual microgel particles attached to an interface. AFM is an excellent tool for this approach.

For applications of such attached particles as sensors or for actuators it is of course necessary to conserve reversibility of the transition. Linear PNIPAM-copolymer chains adsorbed at an interface and in the thin polyelectrolyte multilayers were found to collapse irreversibly [27]. The present study was motivated by the idea that microgels due to their shape stability might conserve reversibility of the transition also in the adsorbed state.

The volume transition of PNIPAM microgels as observed in bulk solution is usually found to be continuous. However, in solution usually the ensemble averaged size of the microgels is followed and therefore it is not clear whether the continuous character of the volume phase transition arises from the polydispersity of the particles (only apparently continuous) or is a property of a single PNIPAM microgel. The present work also aims to answer this question.

2. Materials and methods

2.1. Microgel synthesis and characterization

N-isopropylacrylamide (NIPAM; synthesis grade, purity 97%), *N*,*N*′-methylene bis-acrylamide (BIS; synthesis grade, purity 99%), vinylacetic acid (VA; synthesis grade), and potassium persulfate (KPS; purity 99%) were obtained from Sigma–Aldrich. In contrast to macroscopic gels it was shown previously that for microgels re-crystallization of the chemicals does not lead to significantly different particle properties [28] and hence, all chemicals were used without further purification. The microgel preparation is based on the procedure described by Pelton and Chibante [1]. For the synthesis of the particles used here we employed a conventional stirring technique as described elsewhere [29,30]. NIPAM of 0.625 g (5.52 mmol), 0.017 g BIS (0.11 mmol), and the desired amounts of vinylacetic acid (VA) (1 mol%, 5 mol%, 10 mol%, and 15 mol%) were dissolved in 100 ml triple distilled, degassed water. The synthesis was performed under a nitrogen atmosphere. After heating the solution to 343 K, 3.61 mg of potassium persulfate was added to start the polymerisation. The mixture became turbid and reaction proceeded for 4 h at constant temperature. Then the microgel suspension was cooled for 12 h under continued stirring. The final step of the preparation involves extensive dialysis for 20 days against de-ionized water (Milli-Q) in order to remove the unreacted monomers and other low molecular weight impurities. Microgel particles were lyophilized for storage purposes. Freeze drying does not change the swelling behavior of the particles [28] and they can be resuspended without any problem for subsequent experiments.

The effective VA content in the prepared microgels was determined using titration with NaOH (Table 1). Compared to the previously investigated PNIPAM-*co*-acrylic acid microgels [31] the amount of effectively incorporated acid groups is lower in the present case. It should also be noted here that in contrast to the recently published synthesis by Hoare and Pelton [32] the particles are synthesized without surfactant.

With respect to their shape and polydispersity, the obtained microgel particles were characterized using scanning electron microscopy. For these measurements a suspension of the microgels is left on the surface of the glass slides (Super-Frost Plus, Menzel & Glaser, Germany). To remove excess particles the slides are washed with water at room temperature and then sputtered with gold until a 15 nm gold layer is obtained (for images, see Supplementary data).

2.2. DLS: experimental setup and data analysis

Light scattering measurements were performed using commercial equipment for simultaneous static and dynamic light scattering experiments from ALV-Laservertriebsgesellschaft (Langen, Germany). The light source employed was the green line ($\lambda = 532$ nm) of a Coherent Compass 315M-150 frequency doubled diode pumped solid state laser, operating with a constant output power of 150 mW. Temperature control of the samples better than 0.1 K was achieved using a toluene bath connected to a Lauda RCS6 thermostat. The toluene also served as an index matching bath. The scattered light was detected with a photomultiplier tube (Thorn EMI) mounted on a goniometer arm, operated in single-photon-counting mode. The pre-amplified fluctuating intensity signal was then time auto-correlated using an ALV-5000 multiple τ hardwire correlator (256 channels, first lag time 200 ns). Measurements for each temperature were repeated three times and averaged afterwards.

The normalized electrical field autocorrelation function $g^1(\tau)$ contains the information about the dynamics of the scattering system. $g^1(\tau)$ can be computed from the respective intensity time correlation function $g^2(\tau)$ by the Siegert relation. In the case of a monodisperse ideal sample $g^1(\tau)$ is represented by a single exponential:

Table 1
Titration results for the PNIPAM-*co*-vinylacetic acid microgels with nominal vinylacetic acid 1 mol% (VA1), 5 mol% (VA5), 10 mol% (VA10) and 15 mol% (VA15)

	Nominal VA content [mol]	Titr. NaOH [ml]	titr. NaOH [mol]	Incorporation [%]	Real content [mol%]
VA1	0.23×10^{-5}	0.75	7.5×10^{-7}	32.6	0.33
VA5	1.20×10^{-5}	2.15	2.15×10^{-6}	17.9	0.90
VA10	2.35×10^{-5}	3.20	3.2×10^{-6}	13.6	1.36
VA15	3.52×10^{-5}	5.75	5.75×10^{-6}	16.3	2.45

Given are the expected theoretical molar contents in 30 mg of the material and the contents determined using titration with NaOH. Using these values the effective incorporation of the acid into the particles is calculated.

$$g^1(\tau) = \exp(-\Gamma\tau) \tag{1}$$

with $\Gamma = D^{\mathrm{T}}q^2$, D^{T} = translational diffusion coefficient and q the scattering vector [33–35]. Usually, samples are polydisperse and the decay of the correlation function must be described by a weighted sum of exponentials,

$$g^1(\tau) = \int_0^{+\infty} G(\Gamma)\exp(-\Gamma\tau)\mathrm{d}\Gamma, \tag{2}$$

where $G(\Gamma)$ is the distribution function of the relaxation rates. An analysis of this distribution of relaxation rates can be performed using the method of cumulants [36], the analysis by an inverse Laplace transformation of Eq. (2) by the use of the *FORTRAN* program *CONTIN* [37,38], or by the ORT procedure suggested by Glatter [39,40]. From the mean value $\overline{\Gamma}$ one obtains the translational diffusion coefficient D^{T},

$$\overline{\Gamma} = D^{\mathrm{T}}q^2, \tag{3}$$

and the hydrodynamic radius R_{h} making use of the Stokes–Einstein equation. R_{h} is then used to calculate the swelling ratio of the microgels that are defined by

$$\alpha = \frac{V_{\mathrm{collapsed}}}{V_{\mathrm{swollen}}} = \left(\frac{R_{\mathrm{h}}^{313.2\ \mathrm{K}}}{R_{\mathrm{h}}^{288.2\ \mathrm{K}}}\right)^3. \tag{4}$$

2.3. SANS: experimental setup and data analysis

The small angle neutron scattering experiments presented here were carried out at the ''Forschungszentrum Jülich'' using the KWS1 machine. For details of the setup see the respective publications of the FZ Jülich. The neutron wavelength was 7.3 Å for all experiments and the sample to detector distances were chosen to be 1.2 m, 4 m and 8 m, covering a q-range 0.007–0.2 $\mathrm{Å}^{-1}$.

The data were collected using two dimensional multi detectors. These data were corrected for the efficiency of the different detector cells using a water spectrum and then because of the isotropic character of the scattering, they were averaged along the azimuth. After correction for the scattering of the solvent and the empty cell, the data were brought on an absolute scale using a Lupolen standard [42]. After this procedure the data sets obtained for different sample to detector distances overlapped within the experimental error interval and no further adjustment was necessary.

The data were then fitted using the expression

$$I(q) \propto \frac{A}{V}\frac{1}{q^4} + \frac{I(0)_L}{1+\xi^2q^2}. \tag{5}$$

In this equation A is the interfacial area in the scattering volume and V is the scattering volume. Similar phenomenological descriptions of microgels were used before [12,43,44] and yield the network correlation length ξ.

2.4. AFM: experimental methods

The atomic force microscopy data were obtained with a BioScope AFM from Digital Instruments/VEECO equipped with a liquid cell for measurements in aqueous environment. Temperature control was achieved with a home built heating stage below the sample and a commercial temperature controller (Wavelength Electronics Inc.).

Standard microscope slides were cleaned thoroughly and coated with a 100 nm Au layer by thermal evaporation. Two different procedures were used to deposit the microgel particles: either the substrate was dipped into an aqueous solution (0.2 mg/ml) of the particles or a droplet of the same solution was deposited on the substrate and removed it after a waiting time of ≈5 min. The deposition always was done using swollen microgels (solutions at room temperature).

In both cases, the adhesion is unspecific and rather weak. Particles were frequently pushed around during AFM imaging. In order to improve the adhesion and to obtain stable imaging conditions, the Au surface was treated with an air plasma (100 W, 0.1 mbar) for approximately 2 min prior to the deposition of the particles. After the deposition, the samples were rinsed with de-ionized water twice for 15 min in order to wash off the weakly bound particles. This procedure leads to a typical surface coverage between 20% and 40%, as shown in Fig. 3. The preparation parameters were chosen such that there were always regions with isolated particles, which can be analyzed more easily than densely packed overlapping ones. On the scanned area 400–800 particles were adsorbed and simultaneously investigated.

In all measurements the AFM was operated in tapping mode in water at the resonance frequency of approximately 8 kHz. We used standard oxide sharpened contact mode SiN cantilevers from Olympus (OMCL-TR400PSA) with nominal spring constants between 0.02 N/m and 0.08 N/m. The AFM scan rate was chosen between 0.5 Hz and 1 Hz. The free cantilever oscillation amplitude was $A_0 \approx 20$ nm in all measurements. (A constant value is required to ensure constant imaging conditions throughout the experiments.) The setpoint A_{set} for the amplitude feedback loop was set to 95% or more of A_0. Fig. 1 shows the influence of the setpoint A_{set}/A_0 on the apparent equivalent particle radius $R_{\mathrm{equiv}} = (3V/4\pi)^{1/3}$ (V: particle volume).

Obviously, the apparent particle size in the swollen state depends on the setpoint. We attribute this to partial indentation of the tip into the swollen particles. Extrapolating of the data in Fig. 1 to $A_{\mathrm{set}}/A_0 = 1$ suggests that we underestimate the actual particle radius by 10–15% when we image at $A_{\mathrm{set}}/A_0 = 0.95$, which corresponds to an underestimation of the volume in the swollen state of 30–50%. In order to eliminate this dependence on the imaging conditions, all radii and volumes reported in the following were extrapolated to $A_{\mathrm{set}}/A_0 = 1$.

After changing the temperature, the system was allowed to equilibrate for a few minutes. Once the reflected laser beam on the laser diode inside the AFM head ceased to drift, the tapping frequency and amplitude were readjusted in order to ensure identical imaging conditions for all images.

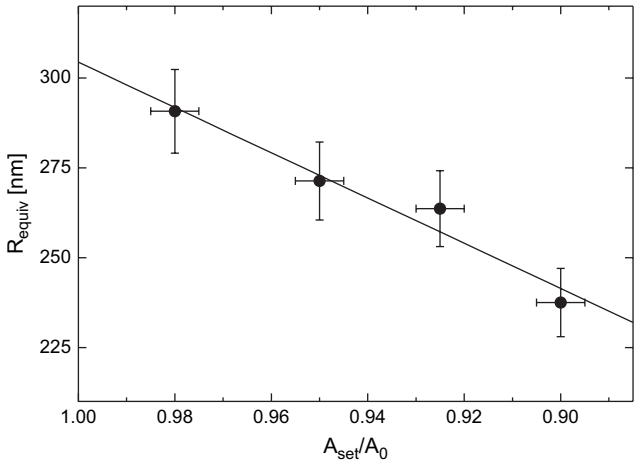

Fig. 1. Influence of the setpoint A_{set}/A_0 of the amplitude feedback loop on the apparent particle radius. The data refer to a swollen VA1 particle at 25 °C. Other particles showed a similar behavior.

In order to analyze the AFM data, the volume V of each particle was determined by numerical integration. In order to do so, the local substrate level had to be determined. This was achieved using a first order flattening and a threshold algorithm in the region around each particle of interest. The uncertainty of various parameters during image processing gives rise to a total error bar for the particle volume of 5–10%. In the collapsed state, this error represents the accuracy of the volume measurement. In the swollen state, however, the error is larger (30–50%) due to tip-induced particle deformation, as discussed above.

For the sake of comparison between DLS and AFM data, we converted the volume measured by AFM into the 'equivalent radius' R_{equiv} of a sphere with the same volume as the adsorbed particles, i.e. $R_{equiv} = \sqrt[3]{3V/4\pi}$.

3. Results and discussion

3.1. Characterization of the microgel particles

3.1.1. DLS

The swelling behavior of the four different microgels was investigated by means of DLS. The microgels are rather large. Therefore, the angular dependence of the decay of the correlation functions was studied first. According to $\Gamma = D^{\mathrm{T}}q^2$ a plot of Γ vs. q^2 should be linear. In Supplementary data the data for the sample VA1 are given.

The linear fit does not go through zero. This can be attributed to growing intra-particle interference at larger scattering angles. However, the effect is small and of comparable magnitude for all prepared PNIPAM-*co*-vinylacetic acid microgels. Hence, all the comparative experiments concerning the swelling behavior were done at a fixed scattering angle of $\theta = 90°$. In all cases the temperature was varied between 15 °C and 40 °C. For each temperature three correlation functions were measured independently and analyzed using CONTIN [37,38] and the method of cumulants [36] (for an example see Supplementary data). Using the method of cumulants the polydispersity is found to be $\leq$10% and also $G(\Gamma)$ reveals the rather narrow size distribution of the prepared microgels. Fig. 2 shows the respective plots of R_h vs. temperature. The shown R_h values are averages of the three measurements. In Table 2 the results from DLS are summarized. The found hydrodynamic radii are in the same range as in previous studies of different copolymer microgels and the swelling ratio α also is in the range expected for particles with a cross-linker content of 2 mol%. Moreover, the swelling capacity does not significantly depend on the content of vinylacetic acid. This finding is in good agreement with the results obtained for PNIPAM-*co*-acrylic acid microgels [31], where even up to acrylic acid contents of 12.5 mol% no change in swelling capacity was observed.

3.1.2. SANS investigation of the network

As already shown in previous studies [12,16,43–45], SANS is a good tool to investigate the local structure of the network inside the microgel particles. Therefore, in the present study we applied SANS to investigate the network mesh size ξ as a function of temperature. Two examples for the obtained series of small angle scattering curves are shown in Fig. 5. The solid lines in the graphs represent fits of the data using a sum of a Porod and an Ornstein–Zernicke term. From these fits one directly obtains ξ. In Table 3 the results for all four samples are given. The found values of ξ are of the same order of magnitude as in previous studies on PNIPAM homopolymer microgel particles [12,13,41,43,44] and are between 3.6 nm and 4.8 nm for the swollen particles. The error of the correlation length ξ as obtained from the nonlinear least squares algorithm used for the data analysis is between 10% and 15%. An increasing amount of vinylacetic acid seems to lead to slightly higher mesh sizes. This effect can be attributed to the slight increase in electrostatic repulsion with increasing VA content of the network. However, at pH values between 5 and 6 the effect is very small, since only a part of the carboxylic acid groups is dissociated. As expected, ξ increases with increasing temperature reaching values of up to 7.5 nm. However, the microgel particles seem to be far away from the critical point and therefore a scaling plot of $\ln(\xi)$ vs. $\ln((T - T_c)/T_c)$ leads to exponents different from the expected value of 0.65 [5] (data not shown). Also this behavior was observed for other microgels [44].

3.2. Swelling behavior of adsorbed particles

While the DLS measurements give informations about the swelling behavior of an ensemble of particles in solution, AFM allows to study individual particles adsorbed on solid substrates.

Fig. 3 shows a large area scan of a typical sample of adsorbed microgel particles. As shown in the inset, the particle size distribution is rather narrow (11%) in agreement with the DLS data.

In order to characterize the swelling behavior quantitatively, we zoomed into a few individual particles. These

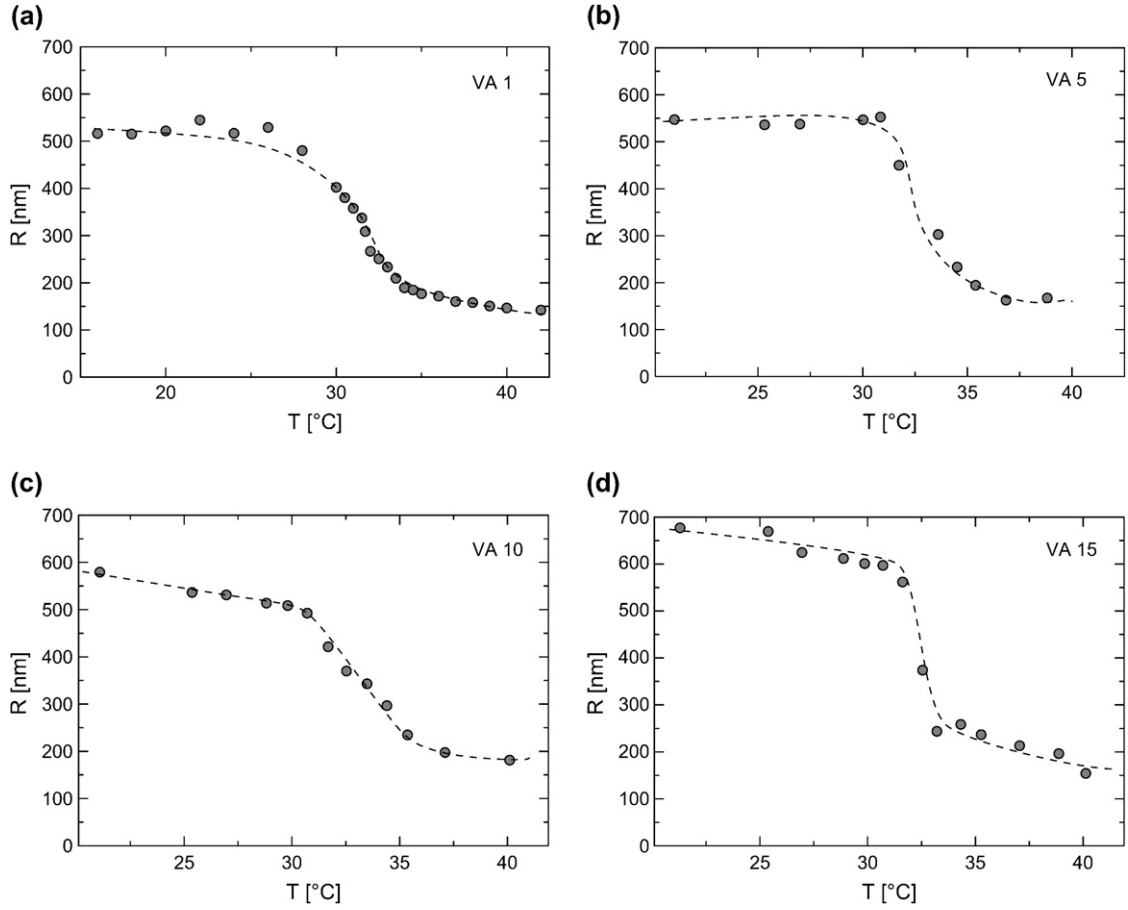

Fig. 2. Swelling curves of the four prepared microgels as obtained by DLS (from VA1 to VA15 (a–d)). The dashed lines are guides to the eye.

particles were then imaged at various temperatures between 25 °C and 40 °C.

Fig. 4 shows a typical example for two VA1 particles. At low temperatures, i.e. in the swollen state (Fig. 4a), the particles appear uniform and smooth. The shape can be approximated by a spherical cap with a rather small 'contact angle' at the edge of $\approx 30°$. The height-to-width aspect ratio is approximately 1:4. Obviously, the particles are deformed substantially upon adsorption onto the surface. AFM imaging of particles in the swollen state is very delicate. In addition to the setpoint-dependence of the particle volume discussed above, AFM images frequently display streaks and stripes, which prevent a quantitative data analysis. Most likely, this is due to the formation of weak bonds between the tip and loosely dangling polymer chains. Typically, this artifact can only be overcome by changing the AFM cantilever. All the data shown below were extracted from artifact-free AFM images, as in Fig. 4. At temperatures above the volume transition, this difficulty is usually absent. This observation is consistent with the idea that loosely dangling polymer chains also collapse at the volume transition temperature and are hence absent at higher temperature.

Table 2
DLS and AFM results for the PNIPAM-*co*-vinylacetic acid microgels with 1 mol% (VA1), 5 mol% (VA5), 10 mol% (VA10), and 15 mol% (VA15) comonomer content

	VA1	VA5	VA10	VA15
R_h (20 °C) [nm]	519	547	536	627
R_h (40 °C) [nm]	141	167	198	197
α	0.02	0.03	0.05	0.02
T_c	31.8	31.8	31.7	32.1
R_{equiv} (25 °C) [nm]	310	270	280	245
R_{equiv} (40 °C) [nm]	160	155	140	140
$\alpha_{interface}$	0.09	0.19	0.13	0.19
$T_c^{interface}$ [°C]	32.7	33.7	32.6	34.0
$\alpha_{interface}/\alpha$	4.5	6.3	2.6	9.5

Table 3
Network correlation lengths ξ of the four investigated microgels as a function of temperature

T [°C]	VA1		VA5		VA10		VA15	
	$I(0)$ [cm^{-1}]	ξ [nm]	$I(0)$ [cm^{-1}]	ξ [nm]	$I(0)$ [cm^{-1}]	ξ [nm]	$I(0)$ [cm^{-1}]	ξ [nm]
25	1.2	3.6	1.9	4.2	2.1	4.8	2.6	4.8
30	2.1	4.6	3.0	5.1	3.6	6.1	4.8	6.4
31	2.4	4.7	3.3	5.2	3.9	6.1	5.4	6.7
31.5	2.6	4.9	3.6	5.5	3.8	5.9	5.5	6.6
32	2.8	5.0	4.3	5.8	4.5	6.5	7.1	7.5

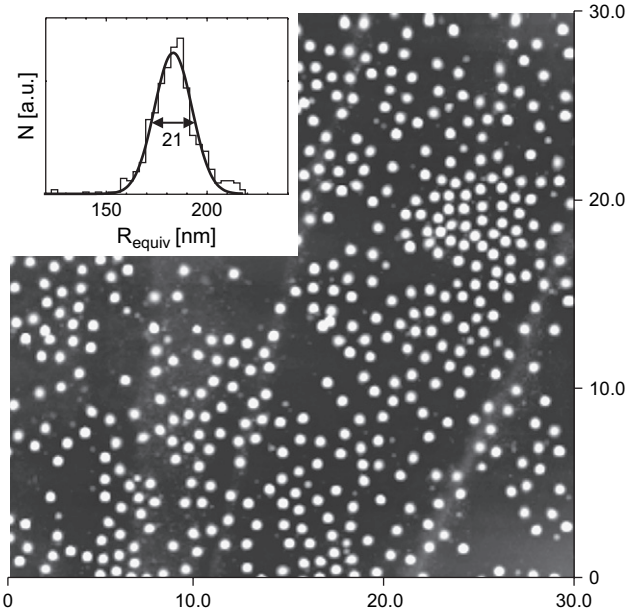

Fig. 3. AFM image (30 × 30 μm) of VA1 microgel particles adsorbed on Au ($T = 35$ °C, gray scale = 300 nm). The width of the Gaussian size distribution is 21 nm or 11% of the mean equivalent radius of $R_{equiv} = 183$ nm. Coverages with VA5, VA10 and VA15 particles look similar.

Upon increasing the temperature the particles' shape changes. Overall, the particles flatten considerably (see Fig. 5). The height-to-width ratio decreases to ≈1:20. The diameter of the particles is only weakly affected by the transition. Obviously, the adhesive bonds to the surface are much stronger than the elastic forces which must be overcome in order to retain the collapsed particles in their flat shape.

A more detailed image of the collapsed particles in Fig. 4c and d reveals a surface pattern for the particles in the collapsed state.

Superimposed on the overall shape of the particles, there appear several "humps" with a characteristic lateral size and height of approximately 100 nm and 10–20 nm, respectively, which are significantly above the substrate roughness (inset of Fig. 6). These features are very reproducible and were observed for all types of particles, independent of the VA content. Once formed during the collapse of a specific particle, the humps remained stable upon further increasing the temperature. Furthermore, their shape was not affected by the settings of the AFM imaging parameters (such as setpoint, imaging velocity and scan size). This robustness suggests that the structures are indeed real. Possible origins will be discussed below.

Both Fig. 4 and the cross-sections in Fig. 5 show that most of the effect occurs in a rather narrow temperature interval between 32 °C and 34 °C. Increasing the temperature further does not affect the shape substantially anymore. For the sake of comparing AFM data to DLS data, we converted the particle volume measured by AFM to the equivalent radius R_{equiv} defined above. Fig. 7 shows swelling curves for four microgel particles with different vinylacetic acid contents. The curves

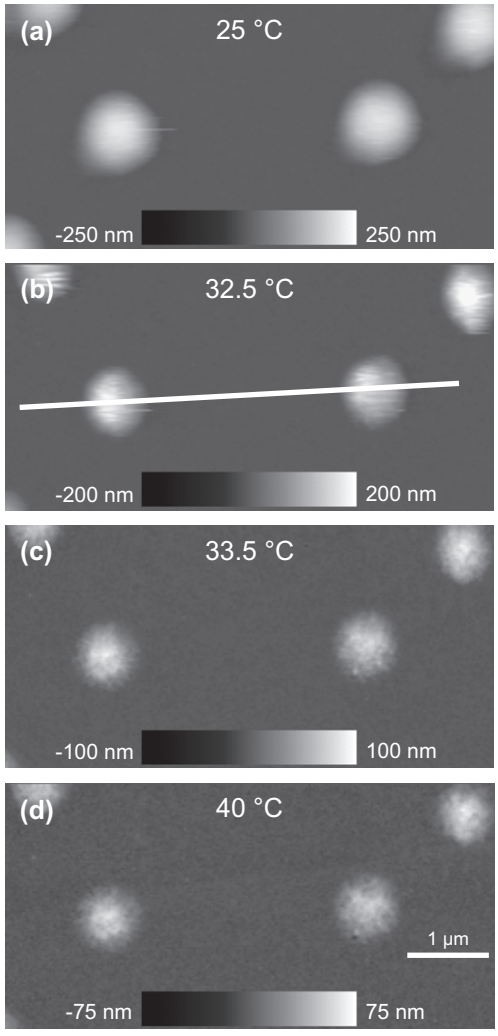

Fig. 4. AFM images of VA1 particles at different temperatures: (a) swollen state (25 °C), (b) beginning of collapse (32.5 °C), (c) almost finished collapse (33.5 °C) and (d) fully collapsed state (40 °C). The line in image (b) indicates the position of the cross-sections in Fig. 5. Note that the range of the gray scale was optimized for each image individually.

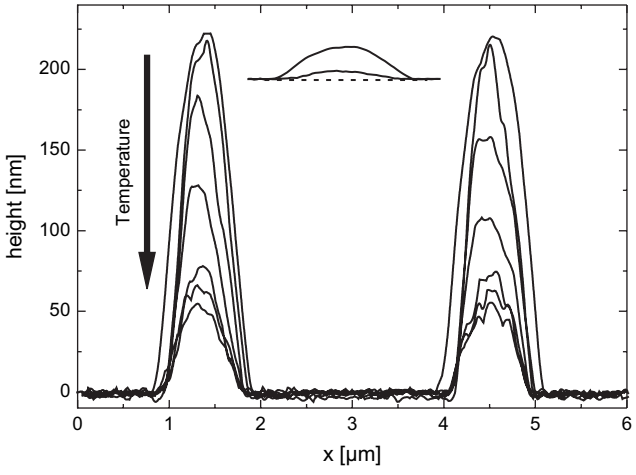

Fig. 5. Cross-sections through AFM images from Fig. 4 for $T = 25$ °C (top curve), 32 °C, 32.5 °C, 33 °C, 33.5 °C, 34 °C and 40 °C (bottom curve). Inset: cross-sections of the left particle with equal scales on both axes for 25 °C and 40 °C to illustrate the actual aspect ratio.

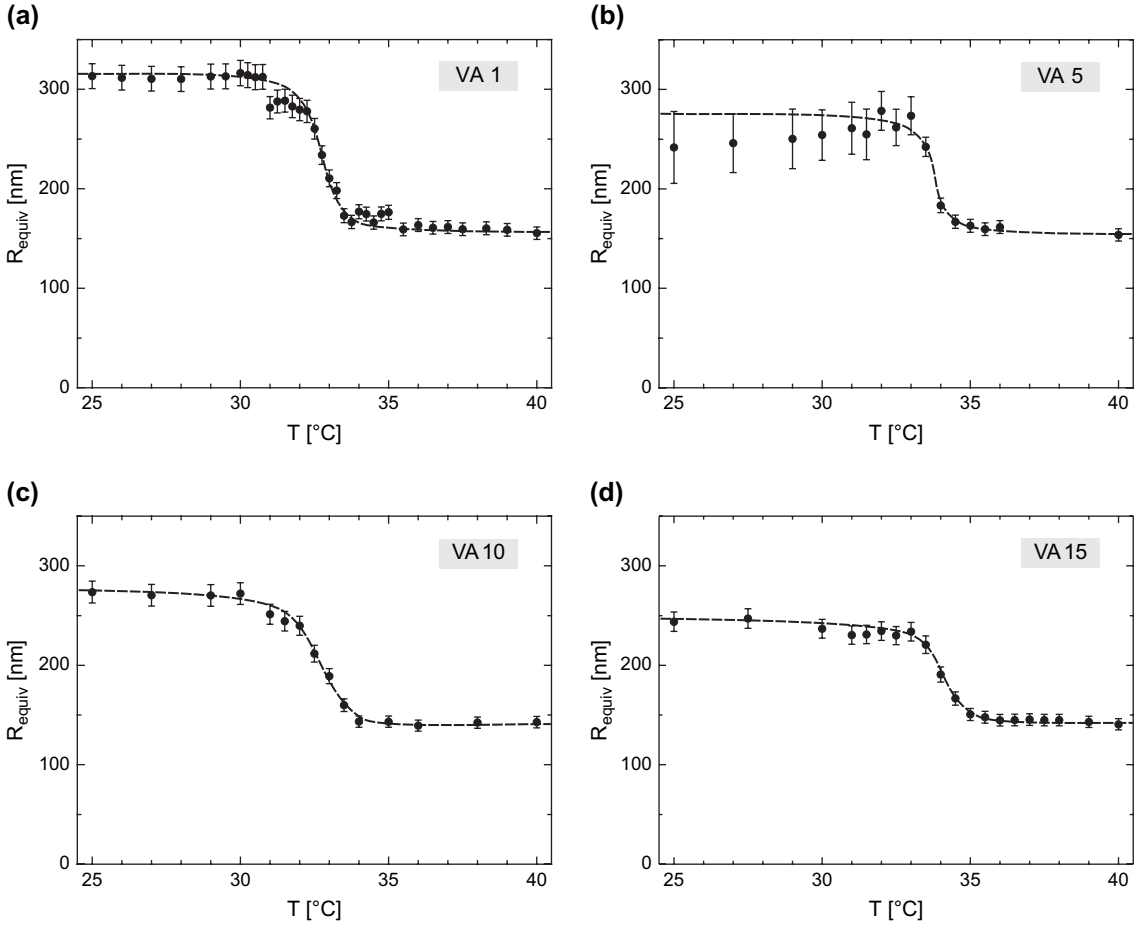

Fig. 6. AFM swelling curves for individual PNIPAM-*co*-VA particles with VA contents of 1 mol%, 5 mol%, 10 mol%, and 15 mol%, respectively. Solid lines are guides to the eye.

are reversible upon heating and cooling.[1] And the continuous character of the transition is also preserved.

For all contents of vinylacetic acid R_{equiv} in the swollen state is approximately 80–90% larger than in the collapsed state, corresponding to a volume increase of a factor of six. The transition temperature, defined by the inflection point of a hyperbolic tangent function fitted to R_{equiv} vs. T is 33 ± 1 °C for all VA contents. The scatter of ± 1 °C arises mainly from particle-to-particle variations of the properties. No systematic trend with respect to the VA content was found. The 80% of the size change takes place within less than 2 °C. Again, the sharpness of the transition is independent of the VA content within the scatter between individual particles.

3.3. Discussion

All our measurements indicate that the volume transition of the particles under investigation takes place at a temperature between 32 °C and 34 °C. There is no systematic dependence of the transition temperature on the VA content within the range studied here, i.e. 2.5% or less. This result differs from

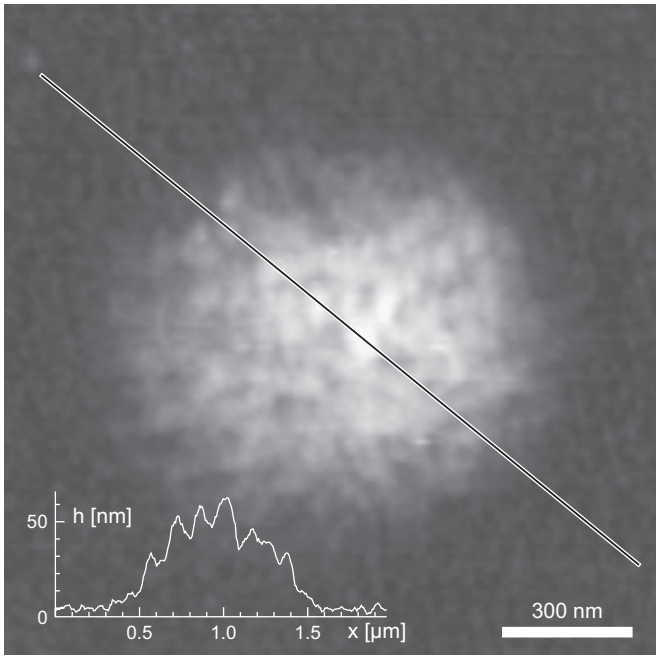

Fig. 7. AFM image of collapsed VA1 particle (T = 35 °C). The cross-section illustrates the internal structure of the particle with humps in the order of 100 nm.

[1] Occasionally, a temperature shift between cooling and heating curve of 0.5–1 °C was observed.

the recent experiments by Hoare and Pelton [32], who found an increase of the transition temperature up to 50 °C for a VA content of 3.3%. These authors attributed the observed VA concentration-dependence to electrostatic repulsion between fully ionized carboxylic acid groups. However, their measurements were performed at pH 10 whereas the pH in our DLS and AFM measurements was between 5 and 6. Hence the carboxylic acid groups are only partially deprotonated and the dependence of the transition temperature on the VA content is reduced — or in fact absent in our experiments. This is also in line with the SANS results where we found only a slight dependence of the network correlation length on the VA content of the particles (Fig. 8). We also note that some details of the synthesis (presence or absence of surfactants) may also affect the microgel particle structure and may thus also contribute to the different behavior.

As major difference between the DLS and the AFM data we also find that the swelling ratio is approximately one order of magnitude smaller for the adsorbed particles in the AFM measurements than for the free particles in solution. Whereas the equivalent radius of the collapsed particles is almost the same as the hydrodynamic radius determined by DLS, the volume of the adsorbed particles in the swollen state is substantially smaller than in the solution. This behavior can be naturally rationalized as follows: the interaction between the PNIPAM chains and the substrate gives rise to a partial collapse upon adsorption. In the swollen state, this reduces the particle volume drastically due to the loose and flexible character of the network. In the collapsed state, the attraction due to the substrate can still deform the particles, however, the enhanced stiffness (compression modulus) prevents a substantial volume change. This scenario is illustrated schematically in Fig. 9.

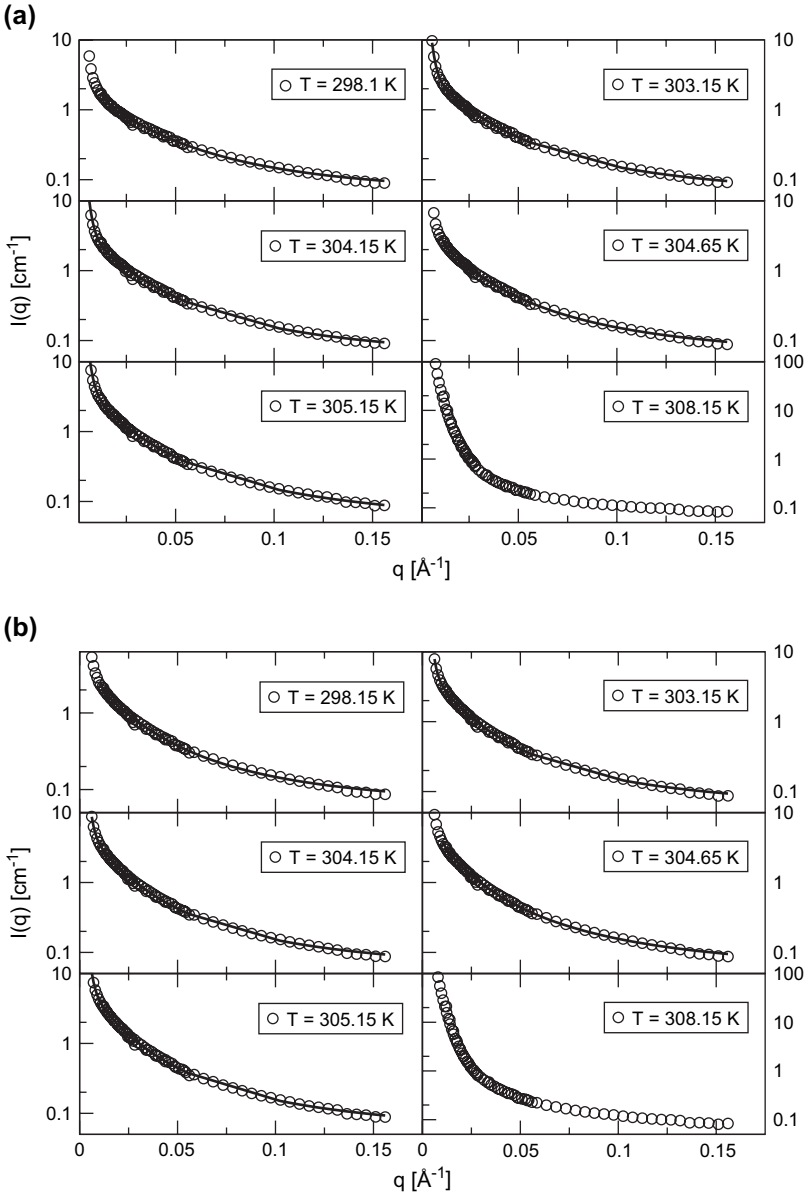

Fig. 8. SANS curves for: (a) the VA1 and (b) the VA10 samples as a function of temperature. The solid lines represent best fits with Eq. (5).

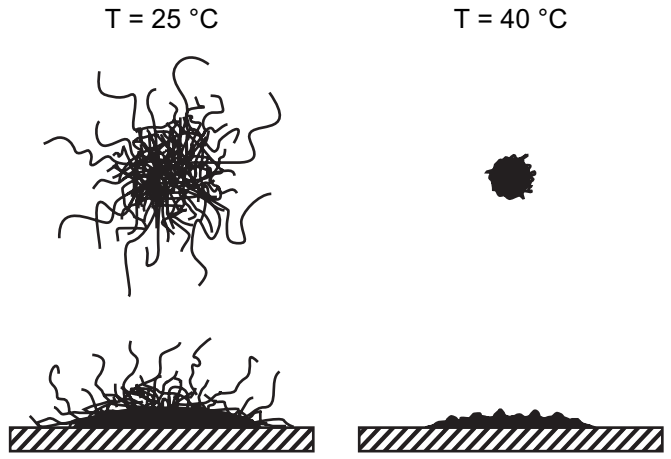

Fig. 9. Model of the shape of a PNIPAM-*co*-AAc particle in liquid (top) and adsorbed to a surface (bottom). For low temperatures (left) the particle shows a soft random coil structure whereas for high temperatures (right) the particles appear in a globular structure.

The initially raised question concerning the continuous character of the volume transition of the microgels can now be answered. The shape of the swelling curve of a single microgel particle in the adsorbed state is very similar to the shape of the curves obtained for the solutions of the microgels. This clearly shows that the smearing and the continuous character do not stem from particle polydispersity, but is a property of an individual microgel. A possible explanation of the smearing of the transition for a single particle would be a rather important heterogeneity of the composition inside the particles and indeed by Richtering et al. it was shown that the particles have a rather inhomogeneous structure internally [45].

In addition to the swelling curves AFM also yielded information about the surface topography of the particles. What is the origin of the observed surface pattern of the collapsed particles? Several possibilities are conceivable. First, one could think that the structure reflects some internal heterogeneity of the gel network. If, for instance, the cross-linking density is strongly inhomogeneous regions with higher cross-linker content would appear stiffer in the AFM. They would be less prone to deformation during the imaging process and could therefore appear as protrusions within a softer and more easily deformable environment. However, if this were the case, the height of the protrusions should depend on the AFM imaging parameters (in particular on the setpoint value), which was not found experimentally. Several years ago, Shibayama et al. [5] found that macroscopic gels of PNIPAM-*co*-acrylic acid display an inhomogeneity on a comparable length scale in the collapsed state. They attributed this feature to a (partial) phase separation of PNIPAM and the comonomer during the synthesis, which leads to a blocky copolymerisation instead of a truly random distribution of comonomers. They argued that under these conditions the volume phase transition takes place in the PNIPAM-rich regions, whereas the acid-rich regions keep a higher water content due to the osmotic pressure of the counter ions. In contrast to Shibayama et al., however, we do not find any substantial dependence of the feature size on the comonomer content, nor do we find any indication of a correlation peak in the SANS data at the corresponding q-value. Thus, we also exclude this interpretation.[2] There is a third possibility, which is related to long protruding polymer chains around the edge of the microgel particles. While these loosely dangling chains sometimes hinder AFM imaging at low temperatures (swollen particles), they should also collapse at the volume transition temperature. In this case, they can form collapsed globules sitting on the surface of the microgel particle. The size of these globules should depend on the average length of the loose chains, i.e. on the cross-linking density, but not on the VA content. The latter explanation is in agreement with the actual experimental observations. Moreover, similar observations of surface structures were already made for PNIPAM homopolymer microgels [43]. In this work PNIPAM particles with a higher cross-linker content and therefore shorter dangling ends were found to exhibit a raspberry like surface pattern in the collapsed state with a characteristic length scale between 30 nm and 50 nm. Length changes of the dangling ends in dependence of the cross-linker content of the particles can be rationalized by the anisotropic distribution of the cross-linker in the microgels leading to a rather compact core and a nearly uncross-linked corona [16].

A fourth explanation is the formation of high molecular weight linear chains during the synthesis. In a recent work Zhou and co-workers found the formation of such chains [47]. Using dialysis these might remain in the samples and can adsorb to the microgel particles during the collapse. This process also would lead to some apparent surface roughness. However, in the work by Zhou et al. the synthesis was done in a different way and we think that in the present study the formation of linear chains is only of minor importance, since no small globules were observed in the AFM experiments and no second contribution can be detected in the DLS experiments.

4. Conclusions

The combination of DLS, SANS, and AFM gives a detailed view at various aspects of the swelling behavior of PNIPAM-*co*-vinylacetic acid microgel particles.

All experiments indicate that the volume phase transition temperature is not influenced by the VA content of the particles and is located between 32 °C and 34 °C.

The AFM experiments clearly show that the volume phase transition of the PNIPAM-*co*-VA microgels is still reversible for adsorbed microgels, but the swelling capacity (given as α) decreases by up to one order of magnitude compared to the swelling ratio in bulk solution. Nevertheless, this effect is still sufficient to construct surfaces with a switchable thickness. Using the deposition of linear block copolymer PNIPAM-*b*-PSS this could not be achieved [27]. Also for applications as actuators the change found in particle size is still sufficiently large.

[2] This is in agreement with the recent work by Hoare and Pelton who argue that block formation during synthesis is present for acrylic acid as well as for methacrylic acid, but not for vinylacetic acid [32,46].

Moreover, the confinement by the solid surface does not influence the transition temperature of the microgels and also the continuous character of the transition is preserved and found to be a single particle property.

In addition, the AFM images reveal the existence of a surface structure of the collapsed microgel particles, which probably can be attributed to the presence of collapsed dangling polymer chains leading to rigid globules on the particle surface. This observation is in line with previous studies on homopolymer particles. The size of these dangling chains and therefore the size of the observed globules depends on the cross-linker concentration used in the particle synthesis. Less cross-linker leads to longer dangling chains.

Acknowledgments

We are grateful to Wim Pyckhout-Hintzen for help with the SANS experiments and to the FZ Jülich for providing the beamtime. L.Z. and F.M. acknowledge funding from the Sonderforschungsbereich 569 'Hierarchic Structure Formation and Function of Organic–Inorganic Nano Systems'.

T.H. acknowledges funding by the EUROCORES program within the project Higher levels of self-assembly of ionic amphiphilic block-copolymers (SONS-AMPHI).

Appendix. Supplementary data

Supplementary data associated with this article can be found in the online version at doi:10.1016/j.polymer.2006.10.026.

References

[1] Pelton RH, Chibante P. Colloids Surf 1986;20:247.
[2] Dusek K. Advances in polymer science. Responsive gels: volume transitions I. 1st ed., vol. 109. Berlin: Springer Verlag; 1993.
[3] Dusek K. Advances in polymer science. Responsive gels: volume transitions II. 1st ed., vol. 110. Berlin: Springer Verlag; 1993.
[4] Shibayama M, Tanaka T, Han CC. J Chem Phys 1992;97:6829–41.
[5] Shibayama M, Tanaka T, Han CC. J Chem Phys 1992;97:6842–54.
[6] Shibayama M, Ikkai F, Inamoto S, Nomura S, Han CC. J Chem Phys 1996;105:4358–66.
[7] Saunders BR, Vincent B. Colloid Polym Sci 1997;275:9–17.
[8] Wu C, Zhou S. J Macromol Sci Phys 1997;B36:345–55.
[9] Dingenouts N, Nordhausen C, Ballauff M. Macromolecules 1998;31:8912–7.
[10] Kratz K, Hellweg T, Eimer W. Ber Bunsen-Ges Phys Chem 1998;102:1603–8.
[11] Duracher D, Elaissari A, Pichot C. Colloid Polym Sci 1999;277:905–13.
[12] Crowther HM, Saunders BR, Mears SJ, Cosgrove T, Vincent B, King SM, et al. Colloids Surf A Physicochem Eng Aspects 1999;152:327–33.
[13] Dingenouts N, Seelenmeyer S, Deike I, Rosenfeldt S, Ballauff M, Lindner P, et al. Phys Chem Chem Phys 2001;3:1169–74.
[14] Gan D, Lyon LA. J Am Chem Soc 2001;123:7511–7.
[15] Hellweg T, Kratz K, Pouget S, Eimer W. Colloids Surf A 2002;202:223–32.
[16] Fernandez-Barbero A, Fernandez-Nieves A, Grillo I, Lopez-Cabarcos E. Phys Rev E 2002;66:051803/1–10.
[17] Pelton R. Adv Colloid Interface Sci 2000;85:1–33.
[18] Nayak S, Lyon LA. Angew Chem Int Ed 2005;44:7686–708.
[19] Hellweg T. In: Marzan LL, Kamat P, editors. Nanoscale materials. Dordrecht: Kluwer Academic Publishers; 2003. p. 209–25.
[20] Tanaka T, Fillmore DJ. J Chem Phys 1979;70:1214–8.
[21] Garcia-Salinas MJ, Romero-Cano MS, de las Nieves FJ. J Colloid Interface Sci 2002;248:54–61.
[22] Senff H, Richtering W. J Chem Phys 1999;111:1705–11.
[23] Senff H, Richtering W. Colloid Polym Sci 2000;278:830–40.
[24] Hellweg T, Dewhurst CD, Brückner E, Kratz K, Eimer W. Colloid Polym Sci 2000;278:972–8.
[25] Debord JD, Lyon LA. J Phys Chem B 2000;104:6327–31.
[26] Lyon LA, Debord JD, Debord SB, Jones CD, McGrath JG, Serpe MJ. J Phys Chem B 2004;108:19099–108.
[27] Steitz R, von Klitzing R. Appl Phys A 2002;74:S519–21.
[28] Kratz, K. Intelligente poly-*N*-isopropylacrylamide-Mikrogele unterschiedlicher chemischer Zusammensetzung. PhD thesis, Universität Bielefeld; 1999.
[29] Kratz K, Eimer W. Ber Bunsen-Ges Phys Chem 1998;102:848–54.
[30] Höfl, S. Eigenschaften neuer copolymer-Mikrogele. Master's thesis, TU Berlin; 2002.
[31] Kratz K, Hellweg T, Eimer W. Colloids Surf A 2000;170:137–49.
[32] Hoare T, Pelton R. Macromolecules 2004;37:2544–50.
[33] Chu B. Laser Light Scattering. New York: Academic Press, Inc.; 1974.
[34] Berne BJ, Pecora R. Dynamic light scattering. New York: John Wiley & Sons, Inc.; 1976.
[35] Schmitz KS. An introduction to dynamic light scattering by macromolecules. New York: Academic Press, Inc.; 1990.
[36] Koppel DE. J Chem Phys 1972;57:4814–20.
[37] Provencher SW. Computer Physics Com 1982;27:213–7.
[38] Provencher SW. Computer Physics Com 1982;27:229–42.
[39] Glatter O. Acta Phys Austriaca 1977;47:83–102.
[40] Glatter O. J Appl Cryst 1977;10:415–21.
[41] Dingenouts N, Nordhausen C, Ballauff M. Ber Bunsen-Ges Phys Chem 1998;102:1594–6.
[42] Poppe A, Willner L, Allgaier J, Stellbrink J, Richter D. Macromolecules 1997;30:7462–71.
[43] Kratz K, Hellweg T, Eimer W. Polymer 2001;42:6531–9.
[44] Kratz K, Lapp A, Eimer W, Hellweg T. Colloids Surf A 2002;197:55–67.
[45] Stieger M, Richtering W, Pedersen JS, Lindner P. J Chem Phys 2004;120:6197–206.
[46] Hoare T, Pelton R. Langmuir 2004;20:2123–33.
[47] Zhou G, Veron L, Elaissari A, Delair T, Pichot C. Polym Int 2004;53:603–8.